



Cite this: *Chem. Commun.*, 2015, 51, 12601

Received 25th June 2015,  
Accepted 1st July 2015

DOI: 10.1039/c5cc05212b

www.rsc.org/chemcomm

## Electroclinic effect in a chiral carbosilane-terminated 5-phenylpyrimidine liquid crystal with 'de Vries-like' properties†

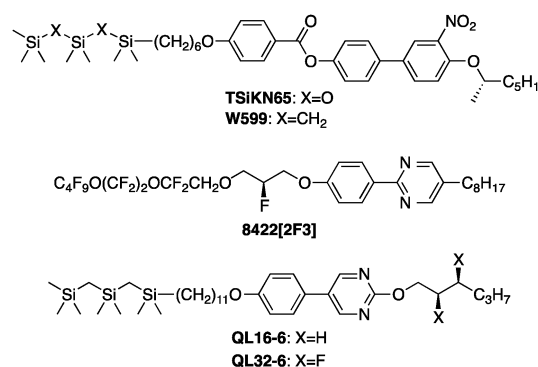
Christopher P. J. Schubert,<sup>a</sup> Carsten Müller,<sup>b</sup> Michael D. Wand,<sup>c</sup>  
Frank Giesselmann<sup>b</sup> and Robert P. Lemieux<sup>\*a</sup>

The chiral carbosilane-terminated liquid crystal 2-[(2*S*,3*S*)-2,3-difluorohexyloxy]-5-[4-(12,12,14,14,16,16-hexamethyl-12,14,16-trisilaheptadecyloxy)phenyl]pyrimidine (QL32-6) undergoes a smectic A\*-smectic C\* phase transition with a maximum layer contraction of only 0.2%. It exhibits an electroclinic effect (ECE) comparable to that reported for the 'de Vries-like' liquid crystal 8422[2F3] and shows no appreciable optical stripe defects due to horizontal chevron formation.

The chiral smectic A (SmA\*) liquid crystal phase is characterized by an analog electro-optical effect known as the *electroclinic effect* that makes it possible to generate a gray scale in display applications on a much faster time scale than a nematic LCD.<sup>1</sup> The SmA\* phase has a diffuse lamellar structure described by a density wave with a period  $d$  corresponding to the layer spacing;<sup>2</sup> the director  $n$  corresponding to the average orientation of long molecular axes is coincident with the layer normal  $z$ . Garoff and Meyer showed that an electric field  $E$  applied parallel to the SmA\* layers induces a uniform molecular tilt relative to  $z$  in a direction orthogonal to  $E$ .<sup>3</sup> This electroclinic effect (ECE) is described by a phenomenological model derived from Landau theory that predicts a linear dependence of the induced tilt angle  $\theta$  on  $E$  at low field strengths; this relationship deviates from linearity when the temperature approaches the transition point  $T_{AC}$  from the orthogonal SmA\* phase to the tilted SmC\* phase.<sup>4,5</sup>

In conventional SmA\* materials, the ECE causes a contraction of the smectic layers that scales with the cosine of  $\theta$  and results in a buckling of the layers into a horizontal chevron structure,<sup>6</sup> which is manifested optically by the appearance of periodic stripe patterns that severely degrade the optical contrast.<sup>7</sup> To solve this problem, a number of groups have investigated the ECE of liquid

crystals with 'de Vries-like' properties,<sup>8</sup> which undergo a SmA\*-SmC\* transition with minimal layer contraction.<sup>9-14</sup> This behavior was explained by de Vries using a 'diffuse cone' model in which mesogens in the SmA\* phase have a tilted orientation and a degenerate azimuthal distribution,<sup>15</sup> although recent theoretical and experimental studies suggest that 'de Vries-like' behavior generally results from an unusual combination of high lamellar order and low orientational order.<sup>16-20</sup> Liquid crystals with 'de Vries-like' properties tend to have unusually large electroclinic susceptibilities, with the field-induced electroclinic tilt accompanied by a significant increase in birefringence that is consistent with an ordering of azimuthal and/or orientational distribution(s).<sup>12,14,21</sup> The ECE of two such materials with first-order SmA\*-SmC\* transitions was recently explained using a generalized Langevin-Debye model, which assumes a random azimuthal distribution of molecules on a fixed tilt cone of angle  $\theta$ , with an orientational distribution in which the tilt  $\theta$  is allowed to vary with the applied field over a prescribed range.<sup>14</sup>



Three SmA\* materials known to have large electroclinic susceptibilities may be considered as *bona fide* 'de Vries-like', *i.e.*, materials that undergo a SmA\*-SmC\* phase transition with an increase in birefringence and a maximum layer contraction of <1%. These are the siloxane-terminated mesogen TSiKN65 and its carbosilane-terminated analogue W599,<sup>10,14</sup> and the 2-phenylpyrimidine mesogen 8422[2F3] from 3M with a chiral

<sup>a</sup> Chemistry Department, Queen's University, Kingston, Ontario, Canada.  
E-mail: rplemieux@uwaterloo.ca

<sup>b</sup> Institute of Physical Chemistry, University of Stuttgart, Pfaffenwaldring 55,  
D-70569 Stuttgart, Germany

<sup>c</sup> LC Vision, LLC, 4150 Darley Avenue, Suite 10, Boulder, CO, USA

† Electronic supplementary information (ESI) available: Synthetic procedures for compound QL32-6, POM textures, tilt angle and birefringence measurements. See DOI: 10.1039/c5cc05212b



perfluoroether chain.<sup>12</sup> The electroclinic susceptibilities of **TSiKN65** and **W599** are remarkably high: tilt angles  $\theta$  of 31° and 25°, respectively, are induced by an electric field of 5 V  $\mu\text{m}^{-1}$  at  $T-T_{AC} = +1$  K. This ECE is accompanied by an increase in birefringence ( $\Delta n = 0.025$  for **TSiKN65**)<sup>21</sup> that is consistent with 'de Vries-like' behavior. Despite the high electroclinic susceptibilities of these compounds, there are structural limitations to their applicability in electro-optical devices. The siloxane end-group in **TSiKN65** is hydrolytically and electrochemically labile,<sup>25</sup> and the lateral nitro group in both compounds is associated with higher rotational viscosities and higher levels of ionic impurities. The electroclinic susceptibility of **8422[2F3]** is somewhat lower than those of **TSiKN65** and **W599** (*vide infra*), but it is chemically inert and the only 'de Vries-like' SmA\* material reported thus far that may be suitable for electro-optical devices based on the electroclinic effect.

We recently developed a molecular design of 'de Vries-like' liquid crystals that combines a nanosegregating carbosilane end-group as SmC-promoting element with either a chloro-terminated alkyl chain or a 5-phenylpyrimidine core as SmA-promoting element.<sup>20,26</sup> For example, the 5-phenylpyrimidine mesogen **QL16-6** undergoes a SmA-SmC transition with a maximum layer contraction of only 0.5% and has a reduction factor  $R$  of 0.23 at the point of maximum layer contraction ( $T-T_{AC} = -6$  K),<sup>27</sup> which makes it one of the best 'de Vries-like' liquid crystals reported heretofore. The profile of relative layer spacing  $d/d_{AC}$  vs.  $T-T_{AC}$  exhibited by these materials typically shows a pronounced negative thermal expansion in the SmA phase that persists on cooling into the SmC phase and counteracts the layer contraction caused by tilting to such an extent that the layer spacing at the SmA-SmC transition is restored. In the case of **QL16-6**, we recently showed that 'de Vries-like' behavior is due to the combined effect of an increase in orientational order and a decrease in bilayer interdigitation with decreasing temperature.<sup>20</sup> In this communication, we report a chiral variant of **QL16-6** that includes a (*S,S*)-2,3-difluorohexyloxy chain, which is known to induce high spontaneous polarizations in FLC mixtures without increasing rotational viscosity.<sup>28</sup> This new mesogen (**QL32-6**) forms SmA\* and SmC\* phases and is comparable to **8422[2F3]** in terms of electroclinic susceptibility and chemical inertness, but is unprecedented in terms of 'de Vries-like' properties.

The chiral mesogen **QL32-6** was prepared by a modification of the synthesis reported for **QL16-6**, as shown in Scheme 1.<sup>20</sup> The chiral (*S,S*)-2,3-difluorohexan-1-ol (**4**) was derived from the chiral epoxide **2**, which was obtained from *E*-2-hexen-1-ol *via* a Sharpless asymmetric epoxidation reaction in 95% ee.<sup>22</sup> The chiral alcohol **4** and the carbosilane-terminated 2-chloro-5-phenylpyrimidine

precursor **6** were then combined *via* a nucleophilic aromatic substitution reaction to give **QL32-6** (see ESI† for all synthetic details). Characterization by polarized optical microscopy (POM) and differential scanning calorimetry (DSC) showed that **QL32-6** forms chiral SmA\* and SmC\* phases at the following temperatures (measured on heating in °C; enthalpies of transition in kJ mol<sup>-1</sup> are in parentheses):

crystal 53 (10) SmC\* 62 SmA\* 77 (7.4) isotropic

The second-order SmA\*-SmC\* transition was observed by POM as the appearance of a Schlieren texture in the homeotropic domain of the SmA\* phase (see Fig. S1 in ESI†). The fan texture of the SmA\* phase turned to a characteristic broken fan texture with a pronounced interference color change that is consistent with an increase in birefringence, as shown in Fig. 1.<sup>8</sup> The SmC\* phase persisted on cooling down to 47 °C.

Measurements of the layer spacing  $d$  as a function of temperature were carried out by small angle X-ray scattering (SAXS). The profile of relative layer spacing  $d/d_{AC}$  vs.  $T-T_{AC}$  for **QL32-6** is compared to that of **QL16-6** in Fig. 2, and shows the same degree of negative thermal expansion in the SmA\* phase, but a less pronounced layer contraction in the SmC\* phase, to the extent that the layer spacing at  $T_{AC}$  is restored at  $T-T_{AC} = -7$  K; the maximum layer contraction of **QL32-6** upon SmA\*-SmC\* phase transition is only 0.2%. The two compounds have comparable tilt angles ( $\theta = 25^\circ$  vs.  $27^\circ$  at  $T-T_{AC} = -10$  K, see Fig. S2 in ESI†), which suggests that **QL32-6** is more 'de Vries-like' than **QL16-6**. Indeed, at the point of maximum layer contraction ( $T-T_{AC} = -3$  K), **QL32-6** has a  $R$  value of only 0.17. By comparison, the 3M material **8422[2F3]** has a maximum layer contraction

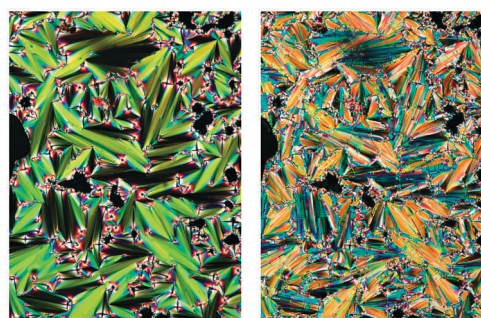
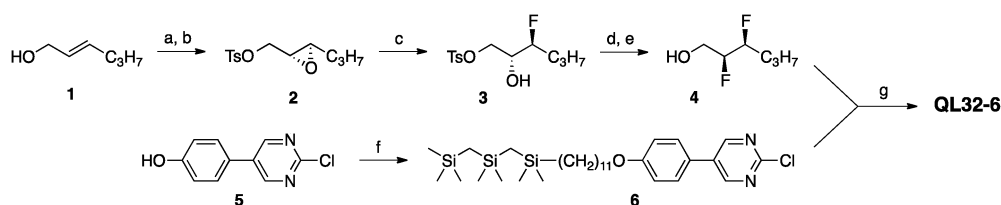


Fig. 1 Polarized photomicrographs of **QL32-6** at 63 °C in the SmA\* phase (left) and at 61 °C in the SmC\* phase (right).



Scheme 1 Reagents and conditions: (a) (–)-Diethyl-*D*-tartrate, Ti(OiPr)<sub>4</sub>, *t*-BuOOH, DCM;<sup>22</sup> (b) *p*-TsCl, pyridine, THF; (c) 70% HF-pyridine, DCM; (d) XtalFluor-E, Et<sub>3</sub>N·3HF, Et<sub>3</sub>N, DCM;<sup>23</sup> (e) Sml<sub>2</sub>, THF;<sup>24</sup> (f) 1-Bromo-12,12,14,14,16,16-hexamethyl-12,14,16-trisilaheptadecane, Cs<sub>2</sub>CO<sub>3</sub>, acetone; (g) (i) **4**, NaH, THF, (ii) **6**.



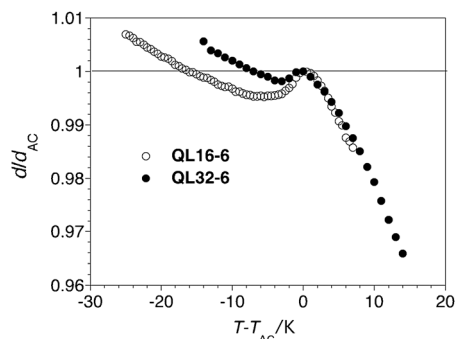


Fig. 2 Relative layer spacing  $d/d_{AC}$  vs. reduced temperature  $T-T_{AC}$  for compounds **QL32-6** (●) and **QL16-6** (○, from ref. 20) measured on cooling from the isotropic phase.

of 0.8% and a  $R$  value of 0.36 at the point of maximum layer contraction ( $T-T_{AC} = -10$  K).<sup>12</sup>

The compound **QL32-6** was aligned in an ITO glass cell with a rubbed nylon alignment substrate and a cell gap of  $3 \mu\text{m}$ . The optical birefringence  $\Delta n$  and electroclinic tilt  $\theta$  were measured as a function of temperature with a rotating analyzer setup described by Langhoff and Giesselmann.<sup>29</sup> The sample was switched by applying alternately a positive and negative electric dc field and the corresponding optical signals were evaluated in terms of phase shift and amplitude to determine the tilt angle and the birefringence simultaneously (see ESI† for details).

The birefringence was first measured at  $E = 0$  over a relatively narrow temperature range about the  $\text{SmA}^*-\text{SmC}^*$  phase transition in order to precisely set  $T_{AC}$  as reference point for all the experiments. As shown in Fig. 3, the birefringence is approximately invariant in the  $\text{SmA}^*$  phase and increases sharply at  $T_{AC}$ , which is consistent with the interference color change observed by POM. Measurements of the electroclinic tilt  $\theta$  in the  $\text{SmA}^*$  phase were performed at five different temperatures above  $T_{AC}$ , from  $T-T_{AC} = +0.2$  to  $+5$  K, with an electric field  $E$  ranging from  $0.1$  to  $20 \text{ V } \mu\text{m}^{-1}$ . As shown in Fig. 4, the  $\theta(E)$  plot is linear at  $T-T_{AC} = +5$  K, but increasingly deviates from linearity as  $T$  approaches  $T_{AC}$ ; at  $T-T_{AC} = +0.2$  K,  $\theta$  reaches values close to  $21^\circ$ . The electroclinic susceptibility of **QL32-6** is about half that of **TSiKN65** but it is comparable to that of **8422[2F3]**: both compounds give a tilt of  $15^\circ$  at  $3 \text{ V } \mu\text{m}^{-1}$  and  $T-T_{AC} = +0.2$  K.<sup>12</sup>

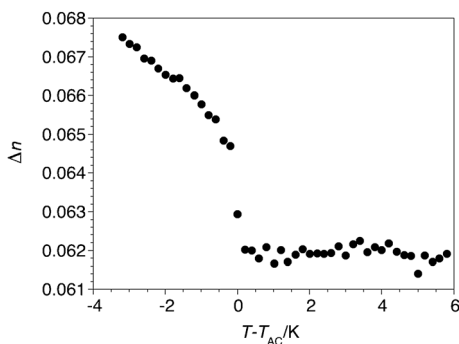


Fig. 3 Birefringence  $\Delta n$  vs. reduced temperature  $T-T_{AC}$  for **QL32-6** measured at  $E = 0$ .

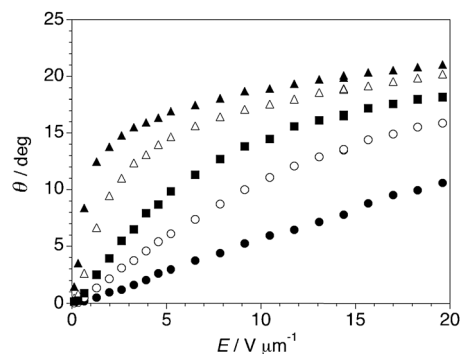


Fig. 4 Electroclinic tilt angle  $\theta$  vs. electric field  $E$  measured in the  $\text{SmA}^*$  phase formed by **QL32-6** at  $T-T_{AC} = +0.2$  K (▲),  $+0.8$  K (△),  $+2$  K (■),  $+3$  K (○) and  $+5$  K (●).

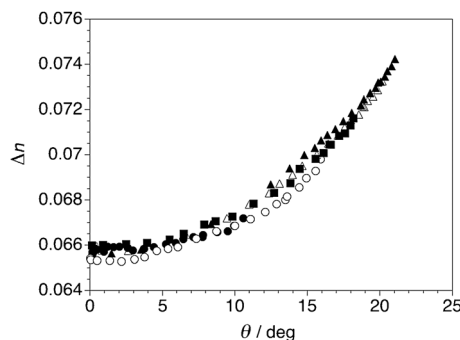


Fig. 5 Birefringence  $\Delta n$  vs. electroclinic tilt angle  $\theta$  measured in the  $\text{SmA}^*$  phase formed by **QL32-6** at  $T-T_{AC} = +0.2$  K (▲),  $+0.8$  K (△),  $+2$  K (■),  $+3$  K (○) and  $+5$  K (●).

The electroclinic tilt observed in the  $\text{SmA}^*$  phase of **QL32-6** is accompanied by an increase in birefringence (see Fig. S3 in ESI†). As shown in Fig. 5, the birefringence increases non-linearly with the electroclinic tilt angle  $\theta$  and is invariant of temperature, so that the  $\Delta n(\theta)$  data sets recorded at five different temperatures fall approximately on the same curve; this behavior, as well as the low absolute values of  $\Delta n$ , were observed for the other three 'de Vries-like' materials described herein.<sup>12,14,21</sup> The unprecedented 'de Vries-like' character of **QL32-6** is reflected by the optical quality of the ECE when compared to **8422[2F3]**. Optical stripe patterns were generated under the same conditions at  $T-T_{AC} = +0.2$  K by applying a  $105$  Hz square wave ac field across  $3 \mu\text{m}$  films at a voltage giving rise to the most intense patterns ( $7.3 \text{ V } \mu\text{m}^{-1}$  for **QL32-6** and  $3.7 \text{ V } \mu\text{m}^{-1}$  for **8422[2F3]**).<sup>30</sup> As shown in Fig. 6, the optical stripe pattern generated by the ECE of **QL32-6** is very subtle, and even less pronounced than the pattern generated by the ECE of **8422[2F3]**. Similar results were obtained on heating the sample to  $T-T_{AC} = +1$  and  $+2$  K (see Fig. S4 in ESI†). Further heating of the sample up to  $T-T_{AC} = +10$  K resulted in the gradual appearance of a stripe pattern at  $E = 0$ , which may be ascribed to a contraction of the smectic layers, *viz.* Fig. 2. Application of a high field of  $15 \text{ V } \mu\text{m}^{-1}$  caused the stripe pattern to disappear (see Fig. S5 in ESI†).<sup>30</sup>

In conclusion, we have shown that a chiral variant of the 'de Vries-like' carboxilane-terminated mesogen **QL16-6** exhibits





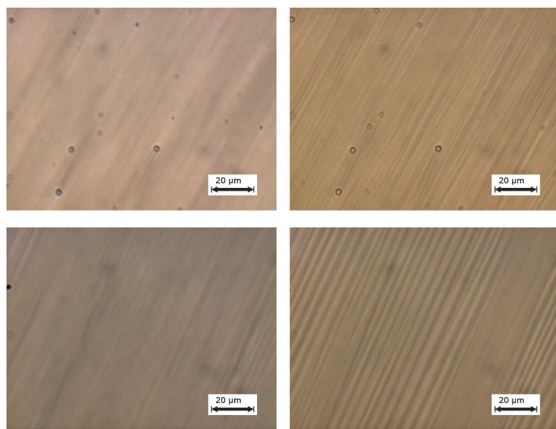


**Fig. 6** Polarized photomicrographs of **QL32-6** (top) and **8422[2F3]** (bottom) in 3  $\mu\text{m}$  ITO glass cells with a rubbed nylon alignment substrate at  $T - T_{AC} = +0.2$  K at  $E = 0$  (left) and with an applied 105 Hz square wave ac field of  $7.3$  V  $\mu\text{m}^{-1}$  (**QL32-6**) and  $3.7$  V  $\mu\text{m}^{-1}$  (**8422[2F3]**).

an electroclinic susceptibility that is comparable to that of the 3M material **8422[2F3]**. Measurements of smectic layer spacing as a function of temperature revealed that it undergoes a  $\text{SmA}^* - \text{SmC}^*$  phase transition with a maximum layer contraction of 0.2%, which corresponds to an  $R$  value of only 0.17. This is reflected by an ECE with improved optical quality over that of **8422[2F3]**, showing no appreciable optical stripe patterns over prolonged electroclinic switching. Given its chemical inertness and lack of a polar nitro group, **QL32-6** is currently the best ECE material suitable for device applications and represents a promising new lead in the development of materials for fast analog electro-optical applications. Ongoing efforts are focused on increasing the electroclinic susceptibility of **QL32-6** via structural modifications and mixture formulation that can broaden the temperature range of the  $\text{SmA}^*$  phase,<sup>31</sup> and will be reported in due course.

We thank the Natural Sciences and Engineering Research Council of Canada and the Deutsche Forschungsgemeinschaft (NSF/DFG *Materials World Network* program DFG Gi 243/6) for support of this work. We also thank Prof Andy Evans for the use of his chiral phase HPLC instrument.

## Notes and references

- (a) C. Bahr, in *Chirality in Liquid Crystals*, ed. H.-S. Kitzerow and C. Bahr, Springer-Verlag, New York, 2001, p. 223; (b) N. A. Clark and S. T. Lagerwall, in *Ferroelectric Liquid Crystals: Principles, Properties and Applications*, ed. J. W. Goodby, R. Blinc, N. A. Clark, S. T. Lagerwall, M. A. Osipov, S. A. Pikin, T. Sakurai, K. Yoshino and B. Zeks, Gordon & Breach, Philadelphia, 1991, p. 84.
- W. L. McMillan, *Phys. Rev. A: At., Mol., Opt. Phys.*, 1971, **4**, 1238–1246.
- S. Garoff and R. B. Meyer, *Phys. Rev. Lett.*, 1977, **38**, 848–851.
- I. Abdulhalim and G. Moddel, *Liq. Cryst.*, 1991, **9**, 493–518.
- F. Giesselmann and P. Zugenmaier, *Phys. Rev. E: Stat. Phys., Plasmas, Fluids, Relat. Interdiscip. Top.*, 1995, **52**, 1762–1772.
- (a) G. P. Crawford, R. E. Geer, J. Naciri, R. Shashidhar and B. R. Ratna, *Appl. Phys. Lett.*, 1994, **65**, 2937–2939; (b) A. G. Rappaport, P. A. Williams, B. N. Thomas, N. A. Clark, M. B. Ros and D. M. Walba, *Appl. Phys. Lett.*, 1995, **67**, 362–364; (c) R. E. Geer, S. J. Singer, J. V. Selinger, B. R. Ratna and R. Shashidhar, *Phys. Rev. E: Stat. Phys., Plasmas, Fluids, Relat. Interdiscip. Top.*, 1998, **57**, 3059–3062; (d) A. Iida, Y. Takahashi and Y. Takanishi, *Liq. Cryst.*, 2010, **37**, 1091–1096.
- (a) J. Pavel and M. Glogarova, *Liq. Cryst.*, 1991, **9**, 87–93; (b) K. Skarp, G. Andersson, T. Hirai, A. Yoshizawa, K. Hiraoka, H. Takezoe and A. Fukuda, *Jpn. J. Appl. Phys.*, 1992, **31**, 1409–1413; (c) R. Shao, P. C. Willis and N. A. Clark, *Ferroelectrics*, 1991, **121**, 127–136.
- J. P. F. Lagerwall and F. Giesselmann, *ChemPhysChem*, 2006, **7**, 20–45.
- F. Giesselmann, P. Zugenmaier, I. Dierking, S. T. Lagerwall, B. Stebler, M. Kaspar, V. Hamplova and M. Glogarova, *Phys. Rev. E: Stat. Phys., Plasmas, Fluids, Relat. Interdiscip. Top.*, 1999, **60**, 598–602.
- M. S. Spector, P. A. Heiney, J. Naciri, B. T. Weslowski, D. B. Holt and R. Shashidhar, *Phys. Rev. E: Stat. Phys., Plasmas, Fluids, Relat. Interdiscip. Top.*, 2000, **61**, 1579–1584.
- R. Shao, J. E. MacLennan, N. A. Clark, D. J. Dyer and D. M. Walba, *Liq. Cryst.*, 2001, **28**, 117–123.
- J. P. F. Lagerwall, F. Giesselmann and M. D. Radcliffe, *Phys. Rev. E: Stat., Nonlinear, Soft Matter Phys.*, 2002, **66**, 031703.
- N. A. Clark, T. Bellini, R.-F. Shao, D. Coleman, S. Bardou, D. R. Link, J. E. MacLennan, X.-H. Chen, M. D. Wand, D. M. Walba, P. Rudquist and S. T. Lagerwall, *Appl. Phys. Lett.*, 2002, **80**, 4097–4099.
- Y. Shen, L. Wang, R. Shao, T. Gong, C. Zhu, H. Yang, J. E. MacLennan, D. M. Walba and N. A. Clark, *Phys. Rev. E: Stat., Nonlinear, Soft Matter Phys.*, 2013, **88**, 062504.
- A. de Vries, *J. Chem. Phys.*, 1979, **71**, 25–31.
- M. V. Gorkunov, M. A. Osipov, J. P. F. Lagerwall and F. Giesselmann, *Phys. Rev. E: Stat., Nonlinear, Soft Matter Phys.*, 2007, **76**, 051706.
- K. Saunders, D. Hernandez, S. Pearson and J. Toner, *Phys. Rev. Lett.*, 2007, **98**, 197801.
- S. T. Lagerwall, P. Rudquist and F. Giesselmann, *Mol. Cryst. Liq. Cryst.*, 2009, **510**, 148–157.
- D. Nonnenmacher, S. Jagiella, Q. Song, R. P. Lemieux and F. Giesselmann, *ChemPhysChem*, 2013, **14**, 2990–2995.
- C. P. J. Schubert, A. Bogner, J. H. Porada, K. Ayub, T. Andrea, F. Giesselmann and R. P. Lemieux, *J. Mater. Chem. C*, 2014, **2**, 4581–4589.
- J. V. Selinger, P. J. Collings and R. Shashidhar, *Phys. Rev. E: Stat., Nonlinear, Soft Matter Phys.*, 2001, **64**, 061705.
- T. I. Richardson and S. D. Rychnovsky, *Tetrahedron*, 1999, **55**, 8977–8996.
- A. L'Heureux, F. Beaulieu, C. Bennett, D. R. Bill, S. Clayton, F. LaFlamme, M. Mirmehrab, S. Tadayon, D. Tovell and M. Couturier, *J. Org. Chem.*, 2010, **75**, 3401–3411.
- T. Ankner and G. Hilmersson, *Org. Lett.*, 1999, **11**, 503–506.
- R. J. Mandle, E. J. Davis, C.-C. A. Voll, D. J. Lewis, S. J. Cowling and J. W. Goodby, *J. Mater. Chem. C*, 2015, **3**, 2380–2388.
- Q. Song, D. Nonnenmacher, F. Giesselmann and R. P. Lemieux, *J. Mater. Chem. C*, 2013, **1**, 343–350.
- The 'de Vries-like' character of a smectic liquid crystal may be quantified on a scale of 0 (perfect 'de Vries') to 1 (conventional  $\text{SmA} - \text{SmC}$  transition) at a temperature  $T$  below  $T_{AC}$  by the reduction factor  $R$  according to the equation:  $R = \delta(T)/\theta_{opt}(T) = \cos^{-1} [d_C(T)/d_{AC}]/\theta_{opt}(T)$ , where  $\delta$  is the tilt angle required to give the observed layer contraction  $d_C(T)/d_{AC}$  assuming a model of hard spherocylinders in which the layer contraction scales with the cosine of the tilt angle, and  $\theta_{opt}$  is the optical tilt angle measured by POM.
- Y. Takanishi, Y. Ouchi, H. Takezoe, A. Fukuda, A. Mochizuki and M. Nakatsuka, *Jpn. J. Appl. Phys.*, 1990, **2**, L984–L986.
- W. N. Thurmes, M. D. Wand, R. T. Vohra, K. M. More and D. M. Walba, *Liq. Cryst.*, 1993, **14**, 1061–1068.
- A. Langhoff and F. Giesselmann, *ChemPhysChem*, 2002, **3**, 424–432.
- The intensity of the optical stripe pattern increased with the applied voltage up to an optimum value, and then decreased with further increasing  $E$  up to a value of  $15$  V  $\mu\text{m}^{-1}$ , at which point the stripes vanished (see Fig. S4 in ESI†). This may be due to a weakening of surface anchoring that forces the horizontal chevrons to adopt a quasi-bookshelf structure.
- C. S. Hartley, N. Kapernaum, J. C. Roberts, F. Giesselmann and R. P. Lemieux, *J. Mater. Chem.*, 2006, **16**, 2329–2337.

